2021 International Nuclear Atlantic Conference – INAC 2021
Virtual meeting,Brazil,November 29 – December 2, 2021

ISBN: 978-65-594-1256-3

Development of europium-doped ultrasmall luminescent tin oxide nanoparticles for applications in nuclear medicine.

F. F. S. Salvador[1*], L. H. C. Francisco[1], H. F. Brito[2], M. C. F. C. Felinto [1]

[1]*Nuclear and Energy Research Institute (IPEN), University of Sao Paulo.*
[2]*Institute of Chemistry (IQ) University of Sao Paulo.*
**franfranzotti@gmail.com*

1.Introduction

Understanding the structure and properties of living cells, organs and organisms represent the key challenge for modern biology and medicine, so much so that they have inspired the development of increasingly sophisticated analytical and bioimaging techniques [1]. For example, Cerenkov luminescence imaging (CLI) was introduced a decade ago and is becoming an established imaging modality. Nowadays, applications include preclinical molecular imaging, surgery, external beam radiotherapy, photodynamic therapy and endoscopy. Several reviews focusing on CLI discovery and applications can be found in literature. However, the most intensive CL signal distributes in the ultraviolet and blue range, which is easily scattered and absorbed by biological tissues. The possible applications of CLI are therefore limited by poor penetration and low intensity. As a result, research has focused on how to translate CL into red or NIR photons, thus improving CLI penetration. Various materials have been explored in this regard, including quantum dots and nanocrystals [2]. Lanthanide luminescent bioprobes have many advantages for this propose. For example, inorganic nanoparticles doped with lanthanides have long-lived luminescence (on the order of tens of milliseconds), wide shifts between the excitation and emission bands, high resistance to the photodegradation, and low toxicity [1]. Gao et. al. successfully enhanced CL penetration and intensity by using Y_2O_3:Eu^{3+} NPs. They found that Y_2O_3:Eu^{3+} NPs could, indeed, be excited by CL, resulting in a significantly enhanced fluorescence intensity that was over 3 times better within the detection range of CCD cameras. Besides, CLF (Cerenkov luminescence excited fluorescence) intensity had a positive linear correlation with the radioactivity of ^{68}Ga and a concentration of Y_2O_3:Eu^{3+} NPs [3]. Other proeminent host-matrix are the broadband semiconductor nanocrystals, such as SnO_2 and TiO_2. They are studied for a wide range of applications, ranging from transparent electrodes, chemical sensors, batteries, and photocatalysis to more recent applications in biology and medicine [4]. In fact, SnO_2 NPs are potentially promising in the area of nanomedicine, with antimicrobial, antioxidant and antitumor applications [5].

2.Methodology

In this work, Eu-doped (0.5 and 2 mol%) SnO_2 ultrasmall nanoparticles were prepared from $EuCl_3 \cdot 6H_2O$ and $SnCl_2 \cdot 2H_2O$ precursors by the coprecipitation method using ammonium hydroxide. The precipitate was further aged for two days, and remaining chloride ions were removed by continuous washing of the precipitate with distilled water and followed by a qualitative turbidimetric test with $AgNO_3$. Moreover, the precipitate was dried, yielding $Sn_{1-X}O_2$:Eu X mol% luminescent nanopowders, and further sintered, as a systematic study with increasing heat treatment temperature (ranging from 100-1000 °C, with a set interval

of 300 °C) was also carried out. To assess in vitro cytotoxicity of the prepared nanoparticles, a NIH/3T3 murine fibroblast lineage (ATCC® CRL-1658™) was used. Briefly, cells were cultured in DMEM (Dubelcco's Modified Eagle's Medium) high glucose medium supplemented with 10% Fetal Bovine Serum, 1% antibiotic solution (10,000 UI/mL penicillin, 10 mg/mL streptomycin) and incubated at 37°C with 5% CO_2 for 24h in 96-well microplates ($2x10^4$ cells per well). Nanoparticle solutions were prepared in PBS (Phosphate-buffered saline), sonicated for 30 min, and further diluted in a culture medium. Then, the cells were treated with concentrations of nanoparticles ranging from 0.2 to 500 $\mu g.mL^{-1}$. Additionally, cells not treated with nanoparticles and cells treated with 0.5% Triton™ X-100 were used as negative and positive controls, respectively.

3. Results and Discussion

Structural analysis of the synthesized compounds was first carried out by Powder X-ray Diffraction (PXRD), where the characteristic cassiterite SnO_2 (PDF 41-1445) profile is identified (**Fig. 1a**). Additionally, it is highlighted that peak broadening diminishes with increasing sintering temperature, being related to the number of coherent scattering domains with increasing crystal growth. It is also worth mentioning that no europium oxide by-product was found, indicating the efficiency of the synthesis method to incorporate Eu^{3+} ions into SnO_2 host-matrix. Moreover, crystallite size was estimated for the (110) reflection by the Scherrer method, where line broadening was corrected applying NaCl as a standard reference, yielding values of 1.8, 5.3, 11.9 and 19.6 nm for SnO_2:Eu 0.5 mol% with increasing sintering temperature, and 16.7 nm for SnO_2:Eu 2 mol% at 1000 °C, as higher doping concentrations inhibits crystal growth.

Transmission Electron Microscopy (TEM) images (**Fig. 1b**) revealed ultrasmall spheric-like single-crystal nanoparticles of a few nanometers in size (2-3 nm), where high crystallinity may be identified from well-defined interplanar d-spacing in the nanoparticles. These observations corroborate PXRD data, as crystallite size was estimated to be about 2 nm from a relatively narrow size distribution (**Fig. 1c**) for SnO_2:Eu 0.5 mol% dried at 100 °C. It is worth noting that nanoparticles in this size distribution range are classified as ultrasmall nanoparticles (USNPs), which are of particular interest for nanomedicine, since they exhibit unique physicochemical and pharmacokinetic properties.

The luminescent properties of the prepared materials were investigated by standard luminescence spectroscopy, as excitation spectra (**Fig. 1d**) presented mainly narrow absorption bands assigned to intraconfigurational 4f-4f transitions of the Eu^{3+} ion, where the characteristic $^7F_0 \rightarrow {}^5L_6$ dominated the spectra for SnO_2:Eu materials dried at 100 °C monitored on the 612 nm Eu^{3+} red emission. In contrast, the compounds sintered at higher temperatures (400, 700, and 1000 °C) also exhibited broad ligand-to-metal charge transfer (LMCT) bands owing to $O^{2-} \rightarrow Eu^{3+}$ absorption (monitored at 586 nm), and being is directly associated with the substitution of surface Eu^{3+} ions into Sn^{4+} sites. On the other hand, emission profiles (**Fig. 1e**) of SnO_2:Eu materials dried at 100 °C under direct ion excitation (*e.g.* 394 nm) revealed a characteristic optical behavior of Eu^{3+} luminescence, where intense red emission assigned to the hypersensitive forced electric dipole (FED) $^5D_0 \rightarrow {}^7F_2$ transition is predominant. In contrast, increasing europium substitution into the host-matrix accounted only for the emission spectra presenting only the Eu^{3+} allowed magnetic dipole (MD) transition at around 586 nm, indicating that surface Eu^{3+} ions move to centrosymmetric Sn^{4+} sites. Viability results for NIH/3T3 cells are showcased in (**Fig. 1f**). Cells were submitted to different concentrations of nanoparticles using MTS/PMS assay. Each value in the graph is the mean of three replicates and the error bars show the standard deviation (SD). One-way analysis of variance (ANOVA) followed by Bonferroni's multiple comparison test was used for statistical analysis. The significant differences between the groups treated with nanoparticles and the untreated groups are indicated by * ($p < 0.05$). According to **(Fig. 1f)**, none of the concentrations of SnO_2:Eu^{3+} NPs negatively influenced cell viability within 24h. Thus, the NPs were not able to cause biochemically significant damage on viable cells, and were considered safe at concentrations lower than $500 \mu g.mL^{-1}$.

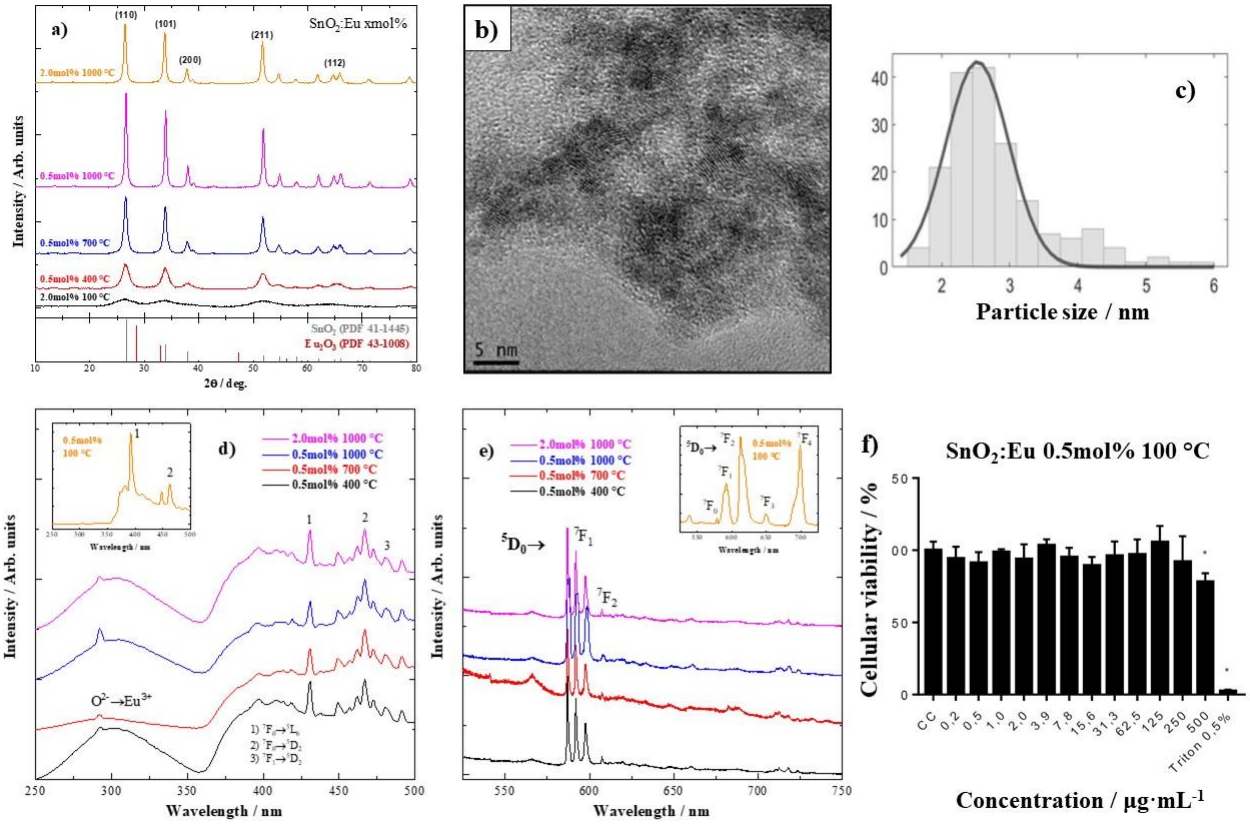

Figure 1: (a) PXRD profile of SnO_2:Eu x mol% (x: 0.5 and 2.0) sintered at different temperatures (100 - 1000 °C) alongside PDF patters of SnO_2 and Eu_2O_3. (b) TEM image of SnO_2:Eu 0.5 mol% 100°C ultrasmall nanoparticles and its (c) particle size distribution. (d) Excitation spectra of Eu-doped SnO_2 materials monitored on the MD (586 nm) and hypersensitive FED (612 nm) transitions of the Eu^{3+} ion. (e) Emission spectra under LMCT (300 nm) and direct ion (394 nm) excitation. (f) Estimated cellular viability from the absorption spectra of MTS assay of cells submitted to different concentrations of SnO_2:Eu 0.5 mol% 100°C nanoparticles.

4. Conclusions

X-ray diffraction profiles indicated the formation of the cassiterite phase, without phase segregation, for all SnO_2:Eu^{3+} nanophosphors. For the materials dried at 100 °C, considerable broadening of the Bragg peaks was observed, since an ideal, perfect and infinite crystal is not satisfied in the nanoscale. The TEM images and histogram corroborate with the PXRD data, revealing the presence of SnO_2 nanocrystals where the average particle size distribution range was in the order of 1.5 to 6 nm. The SnO_2:Eu^{3+} nanoparticles showed emission in the red region between 570 and 720 nm, assigned to the $^5D_0 \rightarrow ^7F_J$ transitions (J = 0-4). For the samples dried at 100 °C, the $^5D_0 \rightarrow ^7F_2$ forced electric dipole transition via direct excitation of the Eu^{3+} ion was dominantly observed. However, for the samples treated at 400, 700 and 1000 °C, the $^5D_0 \rightarrow ^7F_1$ magnetic dipole transition, dominant via indirect excitation above the matrix band gap, was observed via charge transfer. Cell viability tests were performed using the colorimetric method with MTS tetrazolium salt. The results showed that the NPs were not able to cause biochemically significant damage on viable cells (murine fibroblast cell line NIH/3T3), and were considered safe at concentrations lower than 500 $\mu g.mL^{-1}$. These results suggest that the materials are potentially promising in the area of nanomedicine.

Acknowledgements

National Council for Scientific and Technological Development (CNPq); Higher Education Improvement Coordination (CAPES) and Prof. Daniel Perez Vieira.

References

[1] Bunzli, J-C., G. Lanthanide light for biology and medical diagnosis. *Journal of Luminescence*, n. 170, p. 866 – 878 (2016).

[2] Boschi, F.; Spinelli, A. E. Nanoparticles for Cerenkov and Radioluminescent Light Enhancement for Imaging and Radiotherapy. *Nanomaterials*, n. 10, 1771 (2020).

[3] Gao, Y. et. al. Enhanced Cerenkov luminescence tomography analysis based on Y_2O_3:Eu^{3+} rare earth oxide nanoparticles. *Biomed. Opt. Express*. n. 9, p. 6091 – 6102 (2018).

[4] Cojocaru , B. et. al. Nanoscale insights into doping behavior, particle size and surface effects in trivalent metal doped SnO_2. *Scientific Reports*, n.7, v.1, p. 4 – 12 (2017).

[5] Ahamed, M. et. al. Oxidative stress mediated cytotoxicity of tin (IV) oxide (SnO_2) nanoparticles in human breast cancer (MCF-7) cells. *Colloids and Surfaces B: Biointerfaces*, n. 172, p. 152-160 (2018).